Acoustical Physics, Vol. 51, No. 4, 2005, pp. 469–476. Translated from Akusticheskiĭ Zhurnal, Vol. 51, No. 4, 2005, pp. 550–557.

Diffraction Distortion of Surface Acoustic Waves in Crystals

V. I. Cherednick and M. Yu. Dvoesherstov

Lobachevski State University,
pr. Gagarina 23, Nizhni Novgorod, 603950 Russia
e-mail: Dvoesh@rf.unn.ru

Received March 17, 2003

Abstract—A method for the numerical modeling and visualization of the diffraction of surface acoustic waves propagating in anisotropic crystals is described. Examples of two-dimensional wave energy distributions are presented for some crystal orientations widely used in acoustoelectronics. © *2005 Pleiades Publishing, Inc.*

A theoretical analysis of the properties of surface acoustic waves (SAW) propagating in piezoelectric media is usually based on the assumption that the wave front is planar [1, 2]. However, an actual acoustic wave beam, which, as a rule, is excited by an interdigital transducer (IDT), has a finite cross-sectional dimension. Therefore, in the general case, a diffraction of the acoustic wave beam always takes place. If the distance between the IDTs exciting and receiving an electroacoustic surface wave is large, the energy loss owing to the diffraction of the acoustic beam may be considerable. Consequently, the problem of analyzing the diffraction distortion of surface acoustic waves propagating along the surfaces of various piezoelectric crystals and the problem of finding the "optimal" (from the point of view of minimal diffraction distortion) orientations for SAW in these media are important and urgent [1–6].

These problems can be solved using the methods employed in optics [7], i.e., considering the superposition of scalar secondary waves at the point of observation. As indicated in [1], the neglect of the vector character of oscillations is justified for two-dimensional diffraction problems, when the diffraction is considered only in the surface plane of the crystal and the depth dependence is ignored. The essential distinction of the diffraction in anisotropic crystals from the diffraction in optics consists in the fact that the velocity of a surface acoustic wave propagating in an anisotropic medium depends on the direction of propagation. If this dependence can be approximated by a parabola, the diffraction problem can be solved analytically [1, 2]. In the general case, numerical calculations are needed.

In this paper, we present the method and the results of numerical modeling of SAW diffraction in some cuts of quartz (SiO_2), lithium tantalate ($LiTaO_3$), and langasite (LGS) crystals. The amplitude of the resulting wave at an arbitrary point of the crystal surface was calculated as a superposition of waves arriving at this point from various points of the wave source. In this superposition, both plane and cylindrical waves were used. Both variants give practically the same profiles of the transverse amplitude distribution, but, in the case of cylindrical waves, the energy conservation law is additionally obeyed. The dependences of the SAW velocity on the propagation direction in SiO_2, $LiTaO_3$, and LGS piezoelectric crystals were calculated beforehand using the methods described in [8, 9]. The program for calculating the diffraction was done in the Borland C++ Builder visual programming environment. The results of the calculations were automatically passed to the Excel worksheet and were displayed as graphs of two-dimensional wave energy distributions. These graphs clearly show how various cuts and directions in piezoelectric crystals appear from the point of view of diffraction distortion of a SAW. These dependences also contain the quantitative information that allows one to calculate the propagation loss due to the diffraction divergence of an acoustic beam. The visualization of the results of calculation in the form of two-dimensional dependences of radiation energy on the coordinates distinguishes this work from the most recent papers on the same subject, where one-dimensional energy distributions in one coordinate (usually in the transverse one) for some fixed values of the other coordinate are presented (see, for instance, [1–5]). Two-dimensional distributions for quartz, lithium tantalate, and lithium niobate are presented in [6], but they refer to other conditions and orientations.

Let us consider the method for analyzing the diffraction divergence of an acoustic wave beam in more detail. The wave amplitude $A(X, Y)$ at an arbitrary point

1063-7710/05/5104-0469$26.00 © 2005 Pleiades Publishing, Inc.

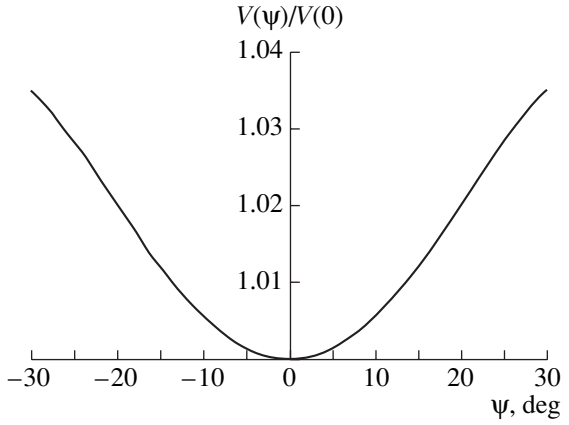

Fig. 1. Normalized phase velocity of a SAW as a function of the third Euler angle ψ in quartz with the (0°, 132.75°, ψ) orientation.

of a plane with the coordinates X, Y can be computed as a superposition of secondary waves [1–6]:

$$A(X, Y) = \int_{-a/2}^{a/2} A_0(Y')K(\alpha)G(R) \times \exp\left[i2\pi\frac{v(0)}{v(\alpha)}R\right]dY'. \quad (1)$$

Here, $X' = 0$, Y' are the coordinates of the source points, $A_0(0, Y')$ is the distribution of the secondary wave amplitude over the source (the input IDT), $G(R) = 1$ for plane waves, $G(R) = \frac{1}{\sqrt{R}}$ for cylindrical waves, $R = \sqrt{X^2 + (Y - Y')^2}$ is the distance from the source point to the point of observation, $\frac{v(\alpha)}{v(0)}$ is the dependence of the normalized phase velocity of a wave on the propagation direction α, $\alpha = \arctan\frac{Y - Y'}{X}$ is the angle of the propagation direction, a is the source width (the aperture), and $K(\alpha)$ is a function that equals unity at $\alpha = 0$ and monotonically decreases with increasing $|\alpha|$ (the simplest variant is $K(\alpha) = \cos(\alpha)$). In [1], the function $K(\alpha) \sim \sin(\alpha)/\alpha$ is used. All of the sizes are normalized by the wavelength λ.

The proposed method makes it possible to model the diffraction of pseudosurface waves as well. It is only necessary to take into account two additional factors: first, the pseudosurface waves attenuate along the direction of propagation and the attenuation coefficient depends on this direction, and, second, these waves do not exist for all spatial orientations. Some examples of the diffraction of pseudosurface acoustic waves are presented in [10]. In the present paper, we only consider the diffraction of surface waves.

The integration in Eq. (1) can be performed analytically if we suppose that $G(R) = 1$ (plane secondary waves), $A_0 = \text{const}$, and the dependence of the SAW velocity v on the direction of propagation is of a parabolic character:

$$\frac{V(\alpha)}{V(0)} = 1 + \frac{1}{2}\gamma\alpha^2. \quad (2)$$

The quantity γ involved in this expression is called the anisotropy parameter [1]. From the analytical theory, it follows that the optimal value of the anisotropy parameter is $\gamma = -1$. For this value of the anisotropy parameter, the diffraction divergence of the acoustic beam is absent and the beam profile remains unchanged at any distance from the aperture [1]. Although the parabolic approximation of the SAW velocity is not always valid, the anisotropy parameter is often used to estimate whether the calculated orientation of a piezoelectric crystal is optimal from the point of view of the diffraction distortion. The anisotropy parameter for an arbitrary specific orientation in a crystal can be calculated by the expression

$$\gamma = \frac{\partial(pfa)}{\partial\Psi}, \quad (3)$$

where

$$pfa = \arctan\left(\frac{1}{v}\frac{\partial v}{\partial\Psi}\right) \quad (4)$$

is the power flow angle.

Here, ψ is the third Euler angle, which determines the direction of SAW propagation in the crystal cut. The crystal cut is defined by the first (ϕ) and second (θ) Euler angles [11].

Note that, in an isotropic medium, the wave velocity does not depend on the propagation direction and the anisotropy parameter γ equals zero. In anisotropic crystals, the behavior of the wave phase velocity strongly depends on all of the three Euler angles determining the orientation in the crystal. For example, Fig. 1 shows the dependence of the normalized SAW phase velocity on the third Euler angle for ST-cut (0°, 132.75°, ψ) quartz in the vicinity of the X direction ($\psi_0 = 0$). The phase velocity is normalized to the velocity corresponding to $\psi_0 = 0$; i.e., this curve can be used for calculations by Eq. (1) ($\alpha = \psi - \psi_0$). Using Eqs. (3) and (4), from the curve given in Fig. 1 for the direction $\psi_0 = 0$, we obtain $\gamma = 0.38$. The positive value of γ corresponds to a greater diffraction divergence than that in the isotropic case; i.e., from the point of view of diffraction distortion, the ST-X quartz is worse than an isotropic medium. Figure 2 displays the calculated two-dimensional isolines of γ for a SAW in the space of the two Euler angles: θ = 0°–180° and Ψ = 0°–180°, at a fixed ϕ = 0° for (0°, θ, Ψ) quartz. As is seen from Fig. 2, there are a number of spatial orientations in which, according

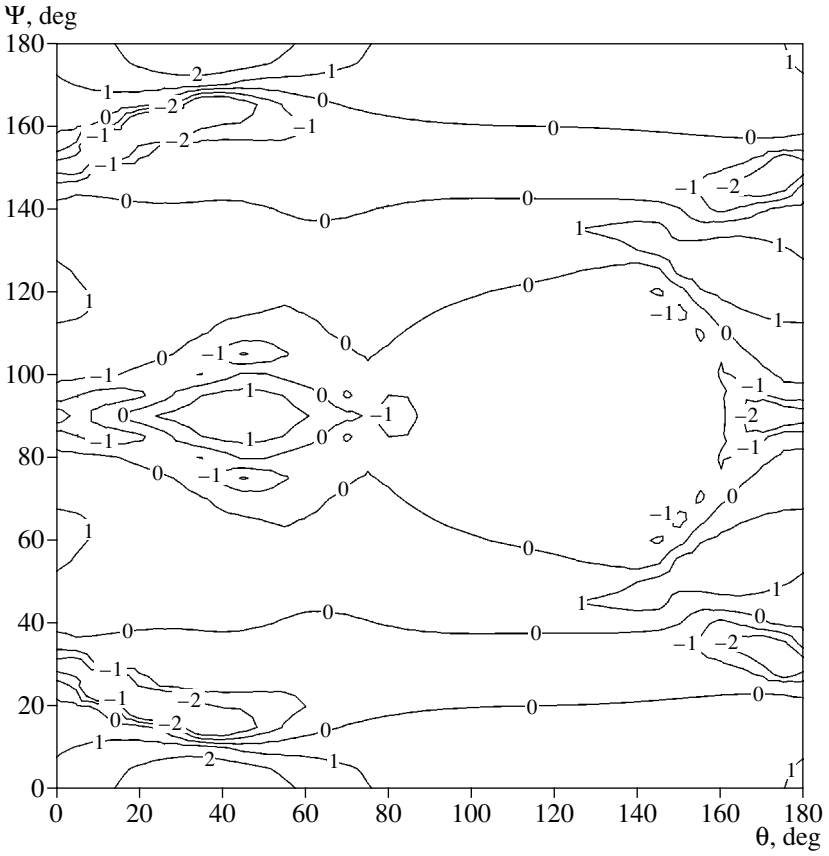

Fig. 2. Dependence of the anisotropy parameter γ on the second (θ) and third (ψ) Euler angles for quartz. The first Euler angle ϕ is equal to zero. The isolines of γ are shown only in the range from –2 to +2.

to the analytical theory, the diffraction distortion of SAW is absent ($\gamma = -1$).

The search for optimal spatial orientations for a SAW in a piezoelectric crystal also includes the following conditions: in the direction found, the SAW should have the minimal power flow angle ($pfa \approx 0$), minimal temperature coefficient of delay ($tcd \approx 0$), maximal electromechanical coupling coefficient (K^2), etc. [2]. The search for the optimal orientation consists in finding the minimum of the objective function Φ_c [12], which is a linear combination of the main parameters of the wave (*tcd*, *pfa*, K^2, γ, etc.) with the corresponding weight coefficients. As a result of such a search, the orientation determined by using the contour maps can be refined to yield the optimal orientation from the point of view of all of the main wave parameters. For instance, for quartz, such an orientation is the orientation near the Euler angles (0°, 45°, 24°). Figure 3 illustrates the dependence of the phase velocity for (0°, 45°, ψ) quartz in the neighborhood of the propagation direction $\psi_0 = 24°$. Near this direction, the velocity reaches its maximum and Eqs. (3) and (4) give $\gamma = -0.79$, which approaches the ideal value $\gamma = -1$. For this direction, $tcd = 0.2 \times 10^{-6}/°\mathrm{C}$, $K^2 = 0.13\%$, $pfa \approx 0$, and the phase velocity is $V = 3.626$ km/s.

If the phase velocity curve for the propagation direction ψ_0 does not have an extremum, then, along with the beam divergence, beam deflection takes place ($pfa \neq 0$).

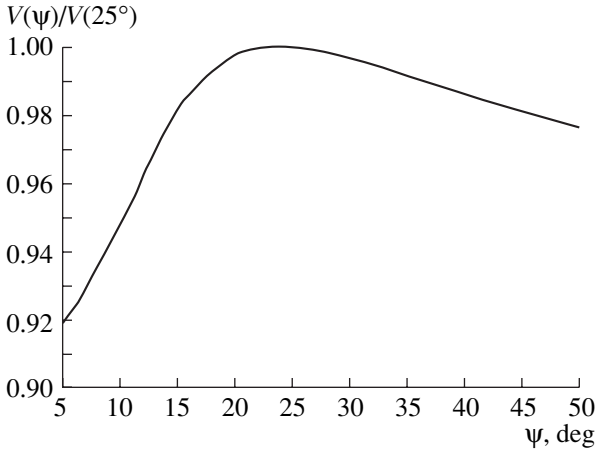

Fig. 3. Normalized phase velocity of a SAW as a function of the third Euler angle ψ in quartz with the (0°, 45°, ψ) orientation.

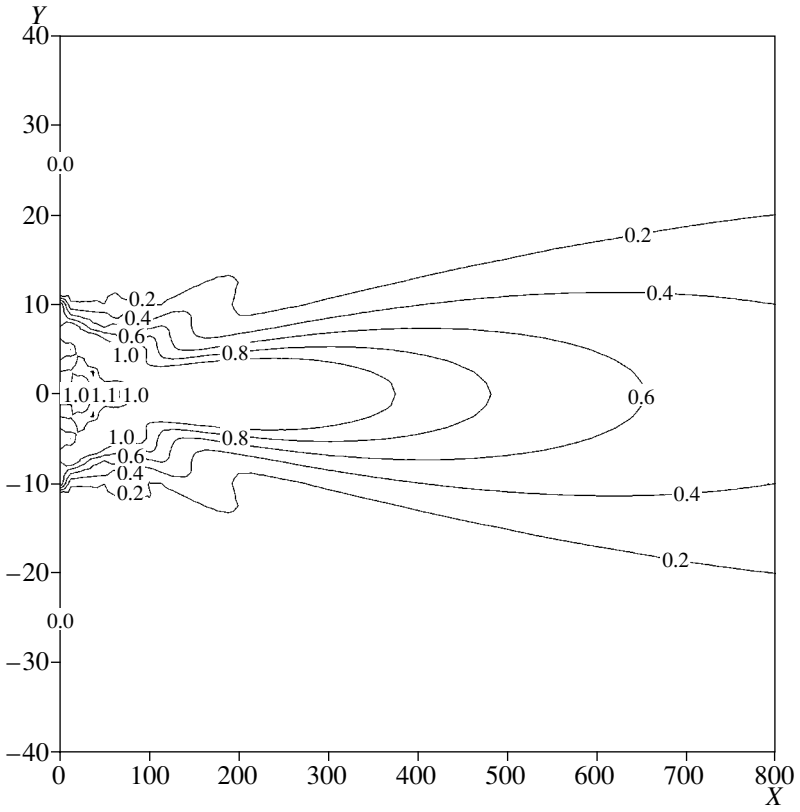

Fig. 4. Isotropic medium, $\gamma = 0$.

For example, in the commonly used orientation of ST + 25 (0°, 132.75°, 25°) quartz, the power flow angle is *pfa* = 5° (see Fig. 1, $\psi_0 = 25°$).

To calculate integral (1), it is necessary first to calculate the wave phase velocity in the angle interval $\Psi_0 \pm 90°$. The values obtained for v were used in the form of tables with a small step in the range from $\psi_0 - 90°$ to $\psi_0 + 90°$. The values at the intermediate points were determined using a linear interpolation.

In the calculation of integral (1), both plane and cylindrical secondary waves were used. Both types of secondary waves gave practically the same profiles of the energy distribution along the transverse *Y* coordinate, but plane waves did not ensure a decrease in the wave amplitude with distance from the source; i.e., they did not satisfy the energy conservation law. They give an incorrect distribution along the *X* propagation direction and do not allow one to obtain a two-dimentional image of the energy distribution. In this case, it is possible to obtain a correct result by applying a special normalization procedure on every line *X* = const. Then, both types of secondary waves give practically the same two-dimensional distributions of wave energy. Some of these distributions are displayed in Figs. 4–9. In all cases, A_0 = const and the aperture is equal to 20 wavelengths. Figures 4–9 show the normalized values of $|A(X, Y)/A_0|^2$, which are proportional to the wave energy.

Figure 4 displays the distribution corresponding to an isotropic medium ($\gamma = 0$). Figures 5–9 represent the energy distributions for the surface acoustic waves corresponding to certain known cuts and orientations in some of the widely used crystals. Figure 5 shows the diffraction pattern for ST-*X* (0°, 132.75°, 0°) quartz. The comparison with Fig. 4 shows that this widely used thermostable cut is rather poor from the point of view of the diffraction divergence. This is caused by the behavior of the SAW velocity in the neighborhood of the propagation direction (the corresponding curve has a minimum). For large distances between IDTs, this orientation is inappropriate. Figure 6 shows the energy distribution for ST + 25 (0°, 132.75°, 25°) quartz. This orientation corresponds to a particular phase relation between the electric potential and the longitudinal displacement of the wave, and, therefore, it can be used for unidirectional IDTs (NSPUDT) [13]. For this orientation, Eqs. (3) and (4) yield $\gamma = -0.22$ and the diffraction divergence is smaller than that in an isotropic medium; however, a 5° deflection of the beam takes place, because the phase velocity curve contains no extremum for this direction. Figure 6 clearly shows how the input and output IDTs should be positioned with respect to each other to avoid energy loss due to this deflection.

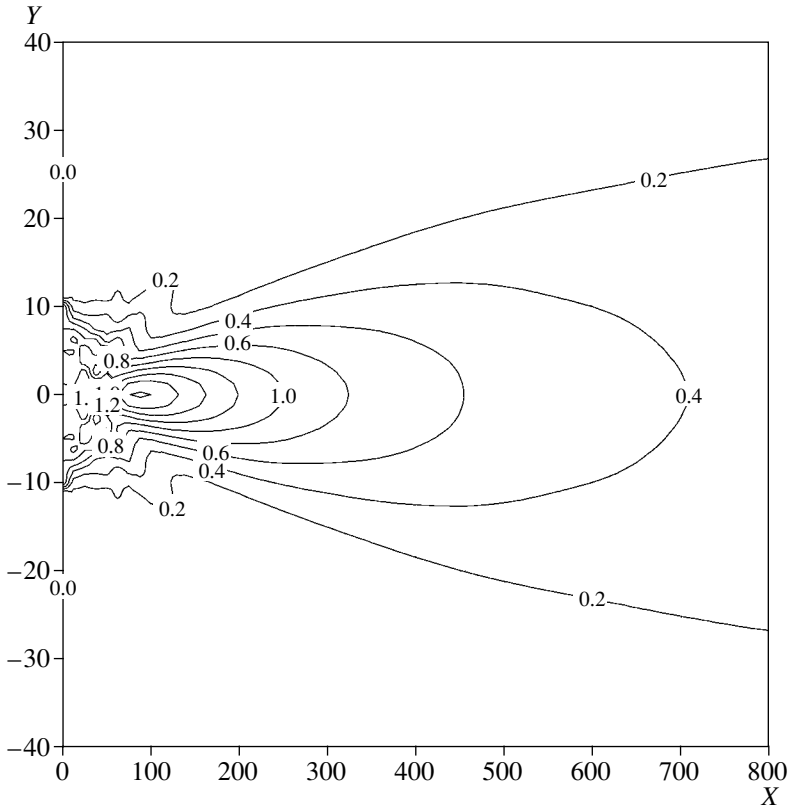

Fig. 5. Quartz with the (0°, 132.75°, 0°) orientation, $\gamma = 0.38$.

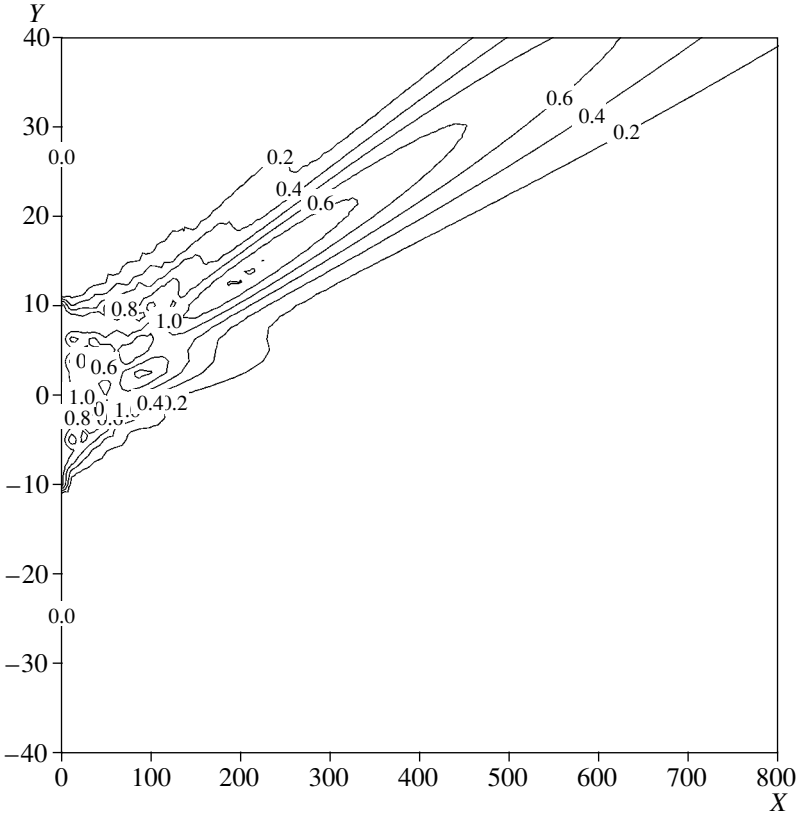

Fig. 6. Quartz with the (0°, 132.75°, 25°) orientation, $\gamma = -0.22$.

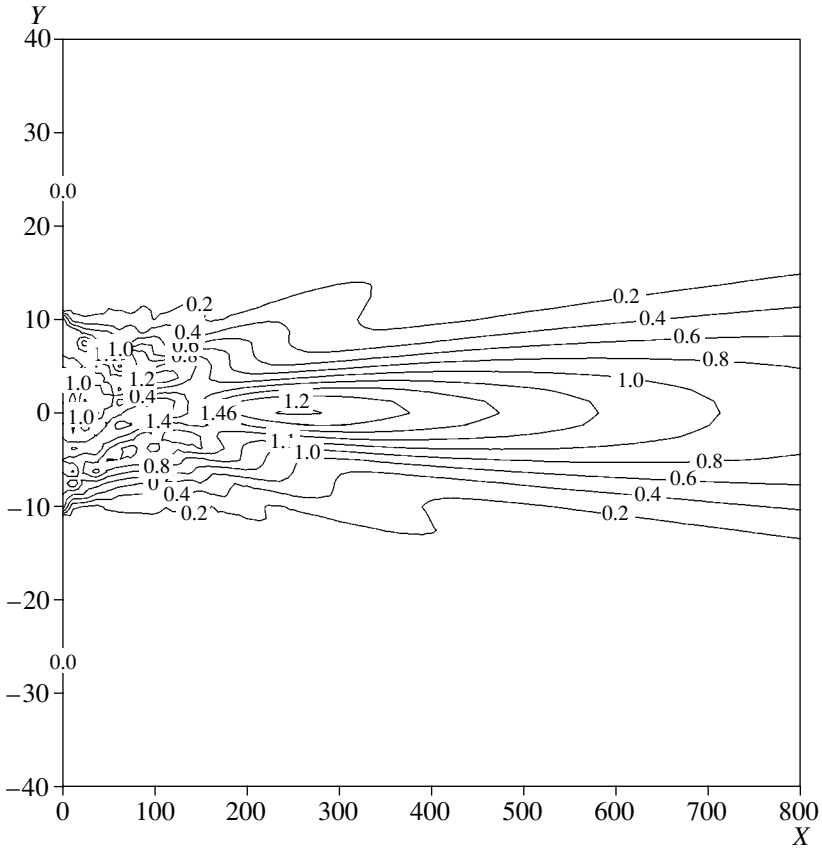

Fig. 7. Quartz with the (0°, 45.1°, 23.95°) orientation, $\gamma = -0.79$.

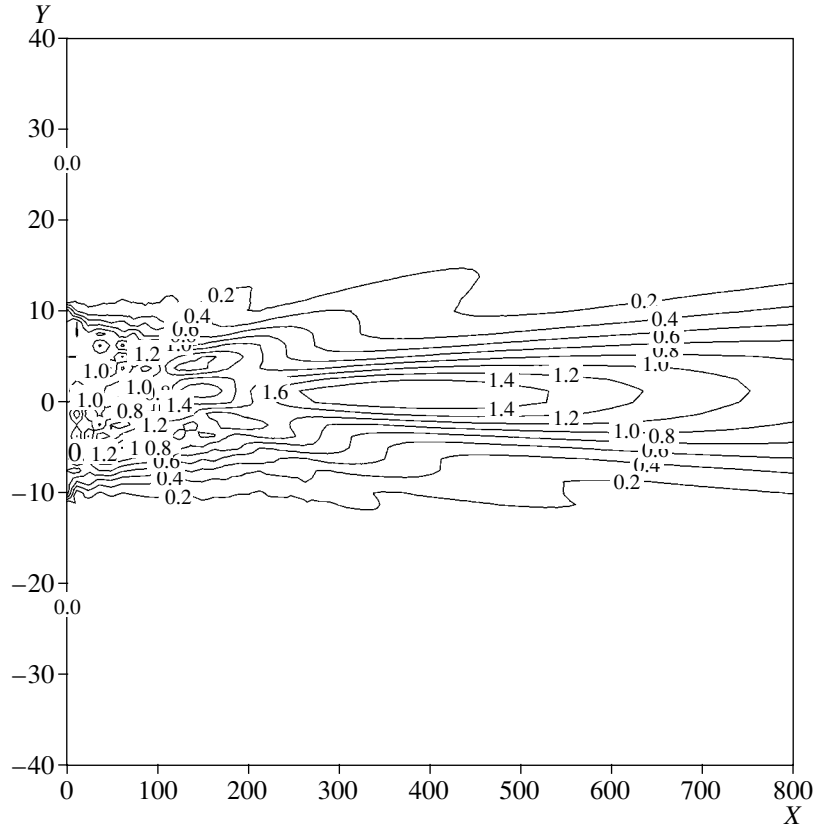

Fig. 8. LGS with the (0°, 140°, 25°) orientation, $\gamma = -1.48$.

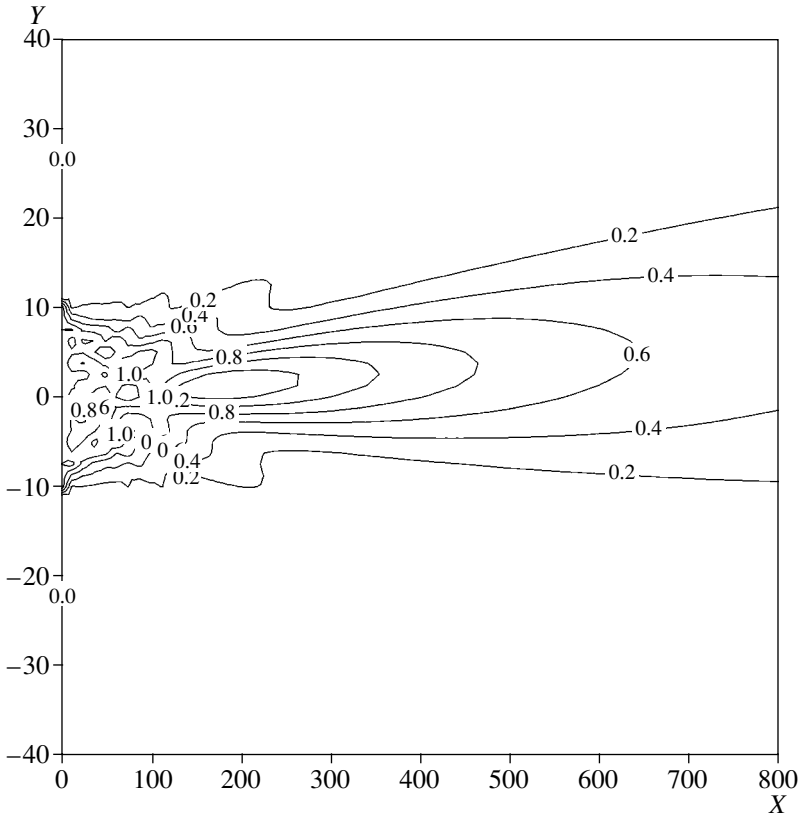

Fig. 9. $LiTaO_3$ with the (90°, 90°, 112°) orientation, $\gamma = -0.3$.

Figure 7 presents the diffraction pattern for a quartz of the (0°, 45.1°, 23.95°) orientation. In the vicinity of this orientation, a SAW has parameters that are close to the optimal ones, in particular, a high thermal stability and a zero power flow angle (the velocity curve has a maximum, see Fig. 3). In addition, for this direction, the anisotropy parameter is $\gamma = -0.79$ and the diffraction divergence is relatively small.

Figure 8 displays the energy distribution for (0°, 140°, 25°) LGS. Near this orientation, all of the wave parameters for this crystal are very good ($v = 2.744$ km/s, $tcd \approx 0$, $K^2 = 0.36\%$, $pfa \approx 0.1°$, and $\gamma = -1.48$). The diffraction divergence is fairly small, as is seen from Fig. 8. However, an asymmetry of the wave beam arises because of the asymmetry of the phase velocity curve near this direction. The material constants for langasite (LGS) were taken from [14].

Finally, Fig. 9 shows the diffraction pattern for (90°, 90°, 112°) $LiTaO_3$. The anisotropy parameter is $\gamma = -0.3$. As is seen from Fig. 9, the wave beam has a small diffraction divergence, but it exhibits a slight deflection, because this direction does not exactly correspond to the maximum of the phase velocity curve ($pfa = 1.2°$). The material constants for $LiTaO_3$ were taken from [15].

Thus, in this paper, we described a method for calculating and visualizing the two-dimensional energy distribution of a propagating surface acoustic wave, which allows one to obtain visual diffraction patterns for any orientation of a piezoelectric crystal of any crystallographic symmetry class. This makes it possible to evaluate different crystal orientations from the point of view of the diffraction loss and the loss associated with the deflection of the power flux of the acoustic beam. In addition, from these distributions, quantitative data can be obtained for calculating the diffraction loss.

REFERENCES

1. *Acoustic Surface Waves*, Ed. by A. A. Oliner (Springer, New York, 1978; Mir, Moscow, 1981).
2. *Surface Wave Filters: Design, Construction and Use*, Ed. by H. Mathews (Wiley, New York, 1977; Radio i Svyaz', Moscow, 1981).
3. R. Milsom, *Proc. IEEE Ultrason. Symp.* (1977), pp. 827–833.
4. G. Kerber and G. Alsup, *Proc. IEEE Ultrason. Symp.* (1977), pp. 834–839.
5. I. Streibl, B. Syrett, and M. Suthers, *Proc. IEEE Ultrason. Symp.* (1983), pp. 62–65.
6. A. Ronnekleiv, *Proc. IEEE Ultrason. Symp.* (2000), pp. 219–222.

7. G. S. Gorelik, *Oscillations and Waves* (Fizmatgiz, Moscow, 1959) [in Russian].
8. M. Yu. Dvoesherstov, V. I. Cherednik, and A. P. Chirimanov, Izv. Vyssh. Uchebn. Zaved. Radiofiz. **43**, 801 (2000).
9. M. Yu. Dvoesherstov, V. A. Savin, and V. I. Cherednik, Akust. Zh. **47**, 847 (2001) [Acoust. Phys. **47**, 682 (2001)].
10. V. I. Cherednick and M. Yu. Dvoesherstov, in *Procceedings of 16 European Frequency and Time Forum, 2002* (St. Peterburg, 2002), p. C107.
11. M. P. Shaskol'skaya, *Acoustic Crystals* (Nauka, Moscow, 1982) [in Russian].
12. M. Yu. Dvoesherstov, S. G. Petrov, V. I. Cherednik, *et al.*, Zh. Tekh. Fiz. **72** (8), 103 (2002) [Tech. Phys. **47**, 474 (2002)].
13. T. Thorvalsson, *Proc. IEEE Ultrason. Symp*. (1989), pp. 820–826.
14. Yu. Pisarevsky, P. Senushencov, B. Mill, *et al.*, *Proc. IEEE International Freq. Control Symp*. (1998), pp. 742–747.
15. G. Kovacs, M. Anhorn, H. Engan, *et al.*, *Proc. IEEE Ultrason. Symp*. (1990), pp. 435–438.

Translated by A. Svechnikov